Finite-State Model-Based Predictive Control with Increased Prediction Horizon for a 7-Level Cascade H-Bridge Multilevel STATCOM

Raúl GREGOR*, Alfredo RENAULT*, Leonardo COMPARATORE*, Julio PACHER*, Jorge RODAS*, Derlis GREGOR†

**Laboratory of Power and Control Systems, † Laboratory of Distributed Systems*

Facultad de Ingeniería, Universidad Nacional de Asunción

Luque, CP 2060, Paraguay

E-mail: {rgregor, arenault, lcomparatore, jpacher, jrodas & dgregor}@ing.una.py

and

Javier MUÑOZ††, Marco RIVERA††

††Department of Industrial Technologies, Universidad de Talca

Talca, CP 747 - 721, Chile

E-mail: {jamunoz, marcoriv}@utalca.cl

***Abstract*—This paper presents a finite-state model-based predictive control technique applied to the three-wire cascade H-bridge multilevel converters for static synchronous compensators. The focus of this paper is to examine the impacts of increasing the prediction horizon on the control performance in terms of reactive power compensation. The proposed approach predicts the future behavior of the control actions considering all possible switching states considering a second step of prediction horizon in order to selects the optimal switching vector by using an optimization process considering a defined cost function. The effectiveness of the proposed control approach is analyzed through simulations.**

***Keywords*—Predictive control, cascade H-bridge converter, reactive power compensation.**

1. INTRODUCTION

Power quality and efficiency issues have been actually consolidated as a scientific topic in the field of electrical engineering due to the technical requirements for grid connection. In recent years, power factor (PF), voltage collapse, unbalance, excessive harmonics, transients and oscillations, have been a major concern in power transmission and distribution systems. Non-linear loads normally produce disturbances in power transmission and distribution systems, causing a high-level harmonic distortion in phase currents and voltages. Moreover, reactive loads produce a low PF, causing an excessive reactive power (VAR) restricting the maximum active power transfer, adding losses to the power transmission and distribution systems affecting its stability and reliability [1]-[3]. Nowadays, several developments of flexible AC transmission system controllers, such as VAR compensators, have been successfully implemented to overcome the aforementioned drawbacks. In recent years, multilevel converters have become a popular alternative to overcome the technological restrictions of the actual semiconductors devices that have limited power ratings [4]. Among all multilevel topologies, the cascaded H-bridge (CHB) multilevel converter is often considered as one of the most suitable configuration for high-power static synchronous compensator STATCOM, especially useful for reactive power compensation [5]. CHB converter-based STATCOM systems have been widely used in high-power applications due to its inherent advantages, such as: reduced switching losses, higher conversion efficiency, modular structure, scalability to extended to more levels and higher number of redundant switching states [6]-[8]. Furthermore, in terms of control strategies, the CHB converter topology increases the degrees of freedom due to its modular feature which allows it to impose an asymmetric control approach. In the mentioned control method certain cells could compensate the PF associated with the fundamental frequency and other cells could control the current harmonic distortion [9], [10]. The main contribution of this paper comparing to previous works is focus on providing a background material about the finite-state model-based predictive control with increased prediction horizon applied to a 7-level cascade H-bridge multilevel STATCOM.

This paper is organized as follows: Section 2 describes the three-wire CHB multilevel STATCOM model. Section 3 discusses the proposed finite-state model-based predictive control technique with increased prediction horizon. Section 4 discusses the simulation results and provides a comparative analysis with a conventional predictive control technique. Finally, concluding remarks are summarized in Section 5.

2. THREE-PHASE CHB STATCOM MODEL

Fig. 1 (a) shows the proposed three-phase 7-level CHB converter-based STATCOM topology, consisting in three cascade H-bridge cells per phase. The different H-bridge cells have an independent DC-link (C_{dc}). Each cell contains four switching devices, resulting in a total of 36 power switchers. Consequently, four switching signals ($S_{f_{ij}}$) are needed in order to controlled each cell, where f represents the phase (a, b and c), i the cell number in the corresponding phase (1, 2 or 3) and j the switching device corresponding to the cell (1, 2 or 3), respectively. Table I shows the allowed combinations of activation signals and the respective output voltages corresponding to the Cell_1 of the phase "a", where C_{dc} is the voltage of the capacitor. Similar allowed combinations are defined for the other cells. Other possible combinations are not permitted because they cause a short circuit in the DC-link of the cell. To avoid this, only two activation signals and they complementary levels are used as shown in Fig. 1 (a) for the particular case of Cell_1.

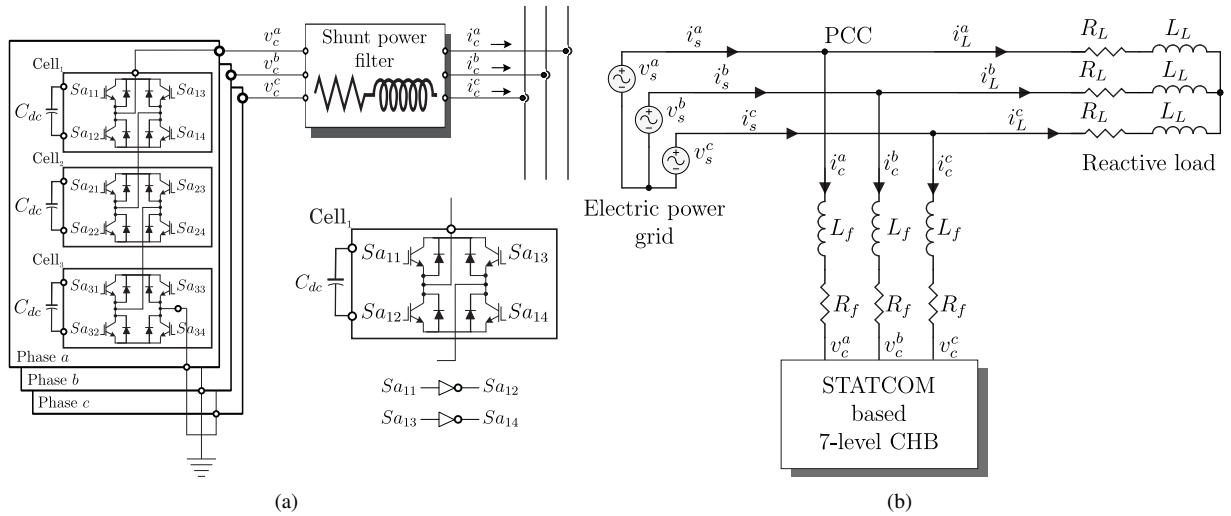

Fig. 1. Propose 7-level CHB converter topology. (a) Three-phase 7-level CHB converter-based STATCOM. (b) CHB converter-based STATCOM connection

TABLE I
ALLOWED COMBINATIONS OF ACTIVATION SIGNALS

Sa_{11}	Sa_{13}	Sa_{12}	Sa_{14}	v_c^a
1	0	0	1	$+C_{dc}$
1	1	0	0	0
0	0	1	1	0
0	1	1	0	$-C_{dc}$

A. CHB converter-based STATCOM model

The dynamic model of the circuit configuration shown in Fig. 1 (b) can be obtained by using Kirchhoff's circuit laws. For modeling purposes, it is assumed that the three-phase voltage sources are balanced and all modules have the same capacitance and voltage in their DC side. The CHB converter-based STATCOM is connected at the point of common coupling (PCC). Applying Kirchhoff's voltage law for the AC side of the STATCOM, the following equations are obtained:

$$\frac{\mathrm{d}i_c^{abc}}{\mathrm{d}t} = \frac{v_s^{abc}}{L_f} - \frac{R_f}{L_f} i_c^{abc} - \frac{n_c S_{f_{ij}} v_{dc}^{abc}}{L_f} \tag{1}$$

$$\frac{\mathrm{d}v_{dc}^{abc}}{\mathrm{d}t} = \frac{S_{f_{ij}} i_c^{abc}}{C_{dc}} - \frac{v_{dc}^{abc}}{R_{dc} C_{dc}} \tag{2}$$

where n_c is the number of cells, R_{dc} is a resistor connected in parallel to the capacitor C_{dc} that concentrates the overall losses in the DC side and the resistor R_f is the parasitic (series) resistance of the inductor L_f.

B. Finite-state predictive model

For multilevel STATCOMs, the differential equation that models the AC side is [11]:

$$\frac{\mathrm{d}i_c^{abc}}{\mathrm{d}t} = \frac{v_s^{abc}}{L_f} - \frac{v_c^{abc}}{L_f} - \frac{R_f i_c^{abc}}{L_f}. \tag{3}$$

The predictive model can be obtained by using a forward-Euler discretization method from the continuous time-domain model represented by (3), which provides the following equation:

$$i_{c\ [k+1]}^{abc} = \left(1 - \frac{R_f T_s}{L_f}\right) i_{c\ [k]}^{abc} + \frac{T_s}{L_f} \left\{ v_{s\ [k]}^{abc} - v_{c\ [k]}^{abc} \right\} \tag{4}$$

where k identifies the actual discrete-time sample, T_s is the sampling time, and $i_{c\ [k+1]}^{abc}$ is a prediction of the STATCOM phase currents made at sample k. However if is considers that the measured currents and voltages at the beginning of the sampling time, which are used in the control loop, are not valid for the end of sampling time, when the microcontroller sends switching states, due to a microprocessor calculation time delay and also to a fast dynamic response of the system it is necessary to carry out a second prediction step as follow:

$$i_{c\ [k+2]}^{abc} = \left(1 - \frac{R_f T_s}{L_f}\right) i_{c\ [k+1]}^{abc} + \frac{T_s}{L_f} \left\{ v_{s\ [k+2]}^{abc} - v_{c\ [k+2]}^{abc} \right\} \tag{5}$$

where $i_{c\ [k+1]}^{abc}$ is calculated from (4) using measured STATCOM currents ($i_{c\ [k]}^{abc}$) and considering the converter voltages ($v_{c\ [k]}^{abc}$) selected by the predictive control in the previous sampling period assuming the $\varepsilon = 2^{2n}$ voltage vectors, where n is the number of H-bridge cells per phase. If $n = 3$, sixty-four possible currents ($i_{c\ [k+2]}^{abc}$) are calculated using the possible voltage vectors $v_{c\ [k+2]}^{abc}$ per phase, which can be applied in next sampling time.

3. PROPOSED CONTROL TECHNIQUE

Fig. 2 shows the block diagram of the proposed finite-state model-based predictive control technique applied to the three-phase 7-level CHB converter-based STATCOM system. In the proposed control approach the predicted errors are computed for each possible voltage vector as:

$$ei_{c\ [k+2]} = i_{c\ [k+2]}^{abc^*} - i_{c\ [k+2]}^{abc} \tag{6}$$

being ei_c the STATCOM current errors in the AC side. The cost function is evaluated sixty-four times by using an optimization process. This cost function provides the ability to define different control criteria incorporating another function objectives. The cost function has been typically defined as a quadratic measure of the predicted error, which can be defined as [12], [13]:

$$g_{\ [k+2]} = \| ei_{c\ [k+2]} \|^2 . \tag{7}$$

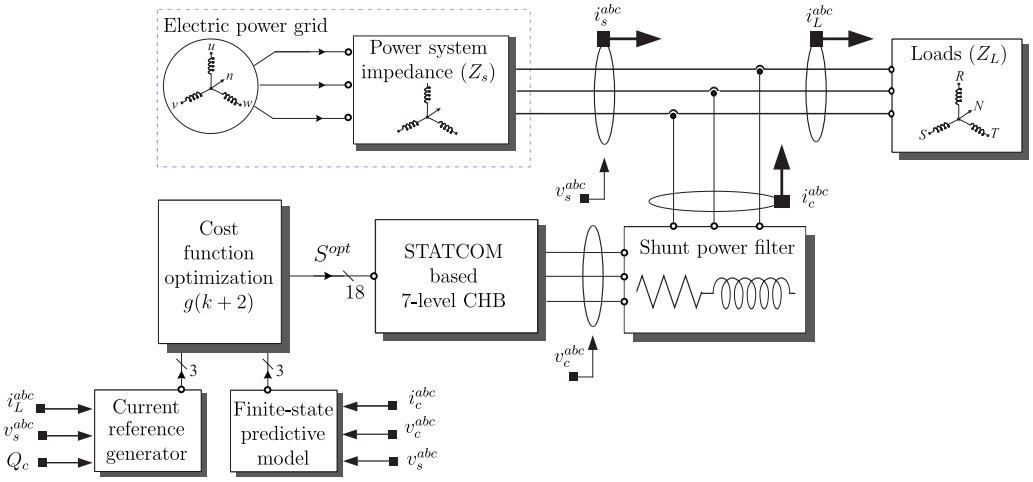

Fig. 2. Block diagram of the proposed control scheme.

A. Reference generation

The instantaneous active and reactive power references are obtained from the Clarke transformation approach in $\alpha - \beta$ reference frame by using the following transformation matrix:

$$\mathbf{T} = \sqrt{\frac{2}{3}} \begin{bmatrix} 1 & -\frac{1}{2} & -\frac{1}{2} \\ 0 & \frac{\sqrt{3}}{2} & -\frac{\sqrt{3}}{2} \\ \frac{1}{\sqrt{2}} & \frac{1}{\sqrt{2}} & \frac{1}{\sqrt{2}} \end{bmatrix}. \tag{8}$$

Applying (8), the $\alpha - \beta$ current references in the AC side of the STATCOM are obtained from:

$$\begin{bmatrix} i_{c\alpha}^* \\ i_{c\beta}^* \end{bmatrix} = \frac{1}{(v_{s\alpha})^2 + (v_{s\beta})^2} \begin{bmatrix} v_{s\alpha} & v_{s\beta} \\ v_{s\beta} & -v_{s\alpha} \end{bmatrix} \begin{bmatrix} P_c^* \\ Q_c^* \end{bmatrix} \tag{9}$$

where the superscript $(^*)$ denotes the reference variables and P_c^* and Q_c^* are the instantaneous active and reactive power references, respectively. In order to allow an unitary power factor at the grid side and considering which ideally the STATCOM do not absorb any active power, the instantaneous power references can be written as:

$$P_c^* = 0 \tag{10}$$

$$Q_c^* = -Q_L = v_{s\alpha} i_{L\beta} - v_{s\beta} i_{L\alpha} \tag{11}$$

being Q_L the instantaneous reactive load power to be compensate by the H-bridge converter-based STATCOM system. The STATCOM phase currents references used in the optimization process are:

$$i_c^{abc^*} = \mathbf{T}^{-1} [i_{c\alpha}^* \quad i_{c\beta}^* \quad 0]' \tag{12}$$

where the superscript $(')$ indicates the transposed matrix.

B. Optimization process

The optimization is performed by exhaustive search over all possible switching vectors of the control action. Considering the scheme shown in Fig. 1 (a), where the number of H-bridge cells per phase ($f \in \{a,\ b,\ c\}$) are three, then each vector $S_{f_{ij}}$ consists in $2n$ choice signals, where $j \in \{1,\ 2,\ 3\}$. During the optimization process, both, the cost function and the predictive model must be computed 64 times at each sampling period to guarantee optimality, since there are 64 possible switching vectors for the case study. These switching vectors represent all possible output voltages of the STATCOM, v_c^a, v_c^b and v_c^c, connected at the PCC point. The output voltages can be represented by the following equation:

$$\begin{bmatrix} v_c^a \\ v_c^b \\ v_c^c \end{bmatrix} = \begin{bmatrix} v_{c1} \\ v_{c2} \\ v_{c3} \end{bmatrix} v_{dc} \tag{13}$$

where v_{c1}, v_{c2} and v_{c3} are the optimal levels of the three-phase 7-level CHB converter-based STATCOM system $(-3, -2, -1, 0, 1, 2, 3)$. The first 15 switching vectors for one phase (a) are shown in Table II.

TABLE II
FIRST 15 SWITCHING VECTORS FOR A THREE-PHASE 7-LEVEL CHB CONVERTER-BASED STATCOM SYSTEM

$S_{a_{ij}}$						η	v_{c1} value
Sa_{11}	Sa_{13}	Sa_{21}	Sa_{23}	Sa_{31}	Sa_{33}		
0	0	0	0	0	0	1	0
0	0	0	0	0	1	2	-1
0	0	0	0	1	0	3	1
0	0	0	0	1	1	4	0
0	0	0	1	0	0	5	-1
0	0	0	1	0	1	6	-2
0	0	0	1	1	0	7	0
0	0	0	1	1	1	8	-1
0	0	1	0	0	0	9	1
0	0	1	0	0	1	10	0
0	0	1	0	1	0	11	2
0	0	1	0	1	1	12	1
0	0	1	1	0	0	13	0
0	0	1	1	0	1	14	-1
0	0	1	1	1	0	15	1
.	.	.	.	.	.	.	.
.	.	.	.	.	.	.	.
.	.	.	.	.	.	.	.

Finally, the optimization algorithm selects the optimum vector S^{opt} that minimizes the defined cost function represented by (7). Algorithm 1 summarizes the optimization process.

4. SIMULATION RESULTS

A MatLab/Simulink simulation environment has been developed to analyze the performance of the proposed predictive controller

Algorithm 1 Optimization algorithm

1. Initialize $J_o^a := \infty, J_o^b := \infty, J_o^c := \infty, \eta := 0$
2. Compute the STATCOM reference currents (Eqn. 12)
3. Compute the first prediction step (Eqn. 4)
4. **while** $\eta \leq \varepsilon$ **do**
5. $\quad S_{f_{ij}} \leftarrow S_{f_{ij}}^{\eta} \ \forall\ i = 1,\ 2,\ 3\ \&\ j = 1,\ 2,\ 3$
6. $\quad$ Compute the second prediction step (Eqn. 5)
7. $\quad$ Compute the tracking error (Eqn. 6)
8. $\quad$ Compute the cost function (Eqn. 7)
9. $\quad$ **if** $J^a < J_o^a$ **then**
10. $\quad\quad J_o^a \leftarrow J^a, \quad S_a^{opt} \leftarrow S_{a_{ij}}$
11. $\quad$ **end if**
12. $\quad$ **if** $J^b < J_o^b$ **then**
13. $\quad\quad J_o^b \leftarrow J^b, \quad S_b^{opt} \leftarrow S_{b_{ij}}$
14. $\quad$ **end if**
15. $\quad$ **if** $J^c < J_o^c$ **then**
16. $\quad\quad J_o^c \leftarrow J^c, \quad S_c^{opt} \leftarrow S_{c_{ij}}$
17. $\quad$ **end if**
18. $\quad \eta := \eta + 1$
19. **end while**
20. Apply the optimum vector $S^{opt} \in \{S_a^{opt}, S_b^{opt}, S_c^{opt}\}$

with increased prediction horizon technique applied to the three-phase 7-level CHB converter-based STATCOM system, considering the electrical parameters shown in Table III.

TABLE III
PARAMETERS DESCRIPTION

PARAMETER	7-Level CHB STATCOM SYMBOL	VALUE	UNIT
Electric frequency of the grid	f_e	50	Hz
Voltage of the electric grid	v_s	310.2	V
Filter resistance	R_f	0.09	Ω
Filter inductance	L_f	3	mH
DC-link voltage	v_{dc}	114	V
	Load parameters		
Load resistance	R_L	23.2	Ω
Load inductance	L_L	55	mH
	Predictive control parameters		
Sampling time	T_s	25	μs
Active power reference	P_c^*	0	W
Ideal Reactive power reference	Q_c^*	$-Q_L$	VAR

Numerical integration using Runge-Kutta method has been applied to compute the evolution of the variables step by step in the time domain. The performance of the proposed finite-state model-based predictive control method has been analyzed in therms of reactive power compensation as well as harmonic distortion considering a 40 kHz of sampling frequency, setting 114 V in the DC side as it is shown in Fig. 1 (a).

Fig. 3 shows a simulation results performed in order to analyze the feasibility of the proposed control technique under steady-state and transient conditions. Fig. 3 (upper) shows a step in the instantaneous reactive power reference where is possible to notice the effect of reactive power compensation. Moreover, Fig. 3 (middle), shows the tracking current dynamic performance for a step change of the reactive power reference. Finally, Fig. 3 (bottom) shows the effect of the grid current when the 7-level CHB STATCOM compensates the reactive power after t = 0.075 s. It can be observed from the

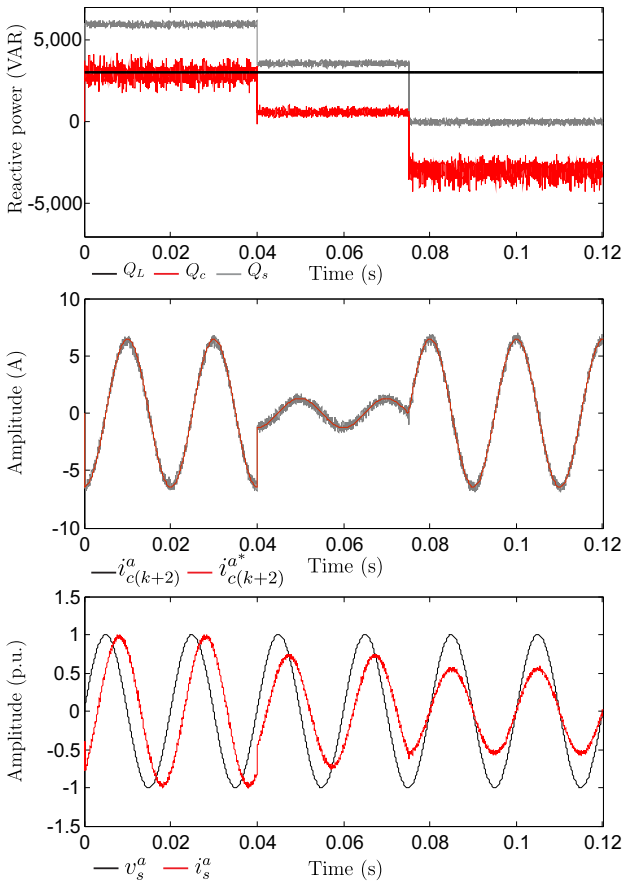

Fig. 3. CHB STATCOM transient response: (upper) reactive power compensation, (middle) tracking current and (bottom) grid voltage and current.

simulation results that the phase of grid current represented in red color, suddenly changes to compensate the reactive power showing a fast dynamic response during the transient.

Next, in order to compare quantitatively the proposed control method with the conventional predictive control technique the mean squared error (MSE) and the total harmonic distortion (THD) are used as figures of merit. The equations are represented by (14) and (15), respectively:

$$\text{MSE}(\Psi) = \sqrt{\frac{1}{N}\sum_{j=1}^{N}\Psi_j^2} \tag{14}$$

$$\text{THD} = \sqrt{\frac{1}{i_1^2}\sum_{i=2}^{N} i_i^2} \tag{15}$$

where N is the number of vector elements, i_1 is the amplitude of the fundamental frequency of the analyzed current, and i_i are the current harmonics.

Fig. 4 shows a comparison analysis between the proposed second prediction step controller and the conventional first prediction step controller considering; (upper) the grid current of the phase a and (bottom) the THD of the analyzed grid current. As shown in Fig. 4 (a) a better performance is obtained using the proposed second prediction step controller mainly in terms of lower THD when the delays are considered in the control equations. This characteristic produce a well-defined discrete current spectra in contrast with the

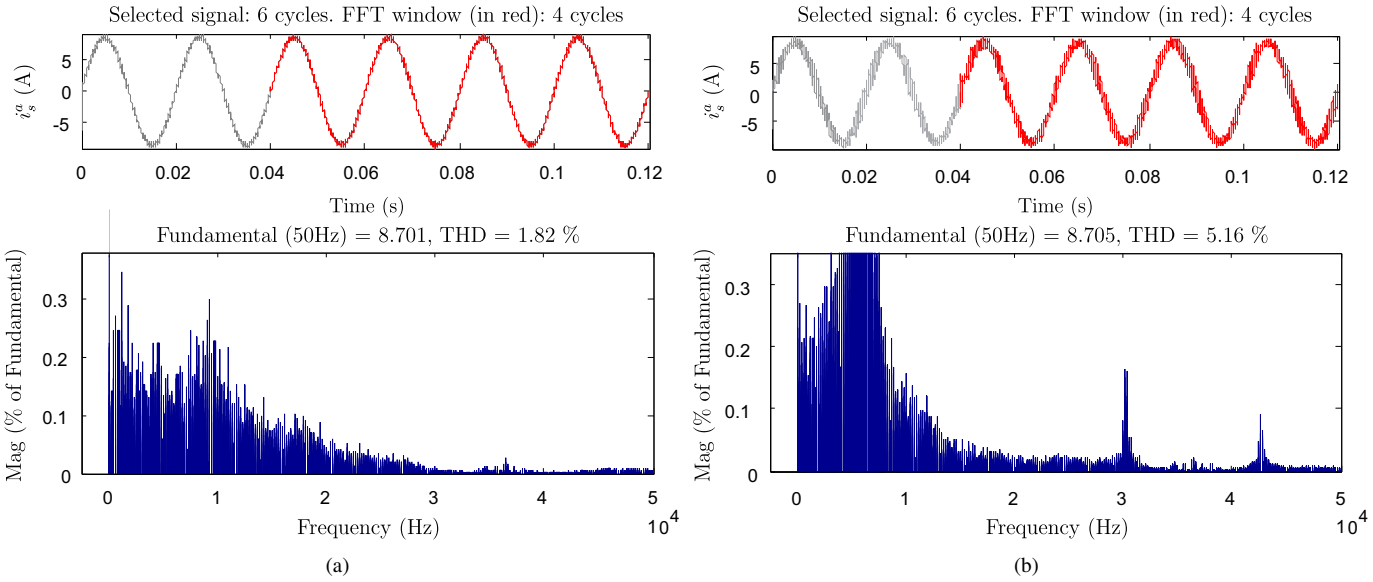

Fig. 4. Comparison performance considering: (upper) the grid current and (bottom) the THD of the grid current. (a) Second prediction step response. (b) First prediction step response.

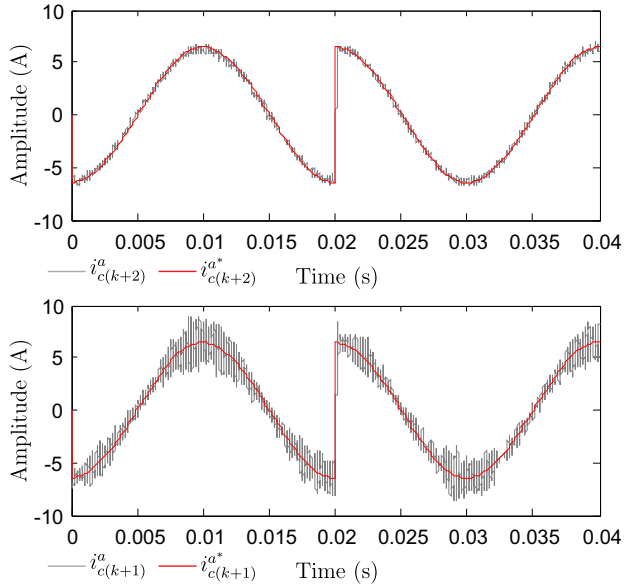

Fig. 5. CHB STATCOM current tracking analysis: (upper) proposed method based on second prediction step and (bottom) conventional method.

conventional one step prediction method. The improvement obtained in the THD performance parameter is about 65% (a drop from 5.16% to 1.82%) using the proposed method, considering the interval where the reactive power is compensated (after 0.05 s).

Furthermore, the second step predictive current control loop is analyzed in more detail to quantify the improvements obtained using the proposed control method in terms of MSE. Fig. 5 shows the dynamic response obtained when a step in the reference reactive power (Q_c) from 3,000 to -3,000 VAR at t = 0.02 s is applied. Under these operating conditions the obtained MSE performance parameters are also reduced using the proposed method, from 0.9816 to 0.3224 which represents an improvement of 67 %. As observed, from the simulation results, the current reference tracking of the proposed method is very good, being even able to reduce the harmonic distortion of the currents without affecting the dynamic response during the transient, which is however very fast.

5. CONCLUSION

In this paper, an enhanced predictive current control technique applied to the three-wire CHB multilevel converters STATCOM has been proposed, analyzed and compared with the conventional one step predictive control approach. The simulation results confirm the capability of the proposed control technique to compensate the instantaneous reactive power and shows that it is possible increased significantly the performance of the control algorithm when is considered the microprocessor calculation time delay defining a second step prediction horizon. A comparative simulation results performed with reference to the conventional method show improvements in terms of total harmonic distortion as well as in terms of mean square error.

ACKNOWLEDGMENT

The authors would like to thank to the Paraguayan Government for the economical support provided by means of a CONACYT Grant project 14-INV-096. In addition, they wish to express their gratitude to the anonymous reviewers for their helpful comments and suggestions.

6. REFERENCES

[1] S. H. Jo, S. Son and J. W. Park, "On Improving Distortion Power Quality Index in Distributed Power Grids," **IEEE Trans. Smart Grid**, vol. 4, no. 1, pp. 586–595, Mar. 2013.

[2] L. K. Haw, M. S. A. Dahidah and H. A. F. Almurib, "A New Reactive Current Reference Algorithm for the STATCOM System Based on Cascaded Multilevel Inverters," **IEEE Trans. Power Electron.**, vol. 30, no. 7, pp. 3577–3588, Jul. 2015.

[3] Y. Neyshabouri, H. Iman-Eini and M. Miranbeigi, "State Feedback Control Strategy and Voltage Balancing Scheme for a Transformerless STATic Synchronous COMpensator based on Cascaded H-bridge Converter," **IET Power Electron.**, vol. 8, no. 6, pp. 906–917, Jun. 2015.

[4] J. Muñoz, et al, "Static Compensators (STATCOMs) in Power Systems," **Control of Multilevel STATCOMs**, ISBN:978-981-287-281-4, pp. 265–311, 2015.
[5] A. Marzoughi, Y. Neyshabouri and H. Imaneini, "Control Scheme for Cascaded H-bridge Converter-Based Distribution Network Static Compensator," **IET Power Electron.**, vol. 7, no. 11, pp. 2837–2845, Nov. 2014.
[6] C. D. Townsend, T. J. Summers and R. E. Betz, "Phase-Shifted Carrier Modulation Techniques for Cascaded H-Bridge Multilevel Converters," **IEEE Trans. Ind. Electron.**, vol. 62, no. 11, pp. 6684–6696, Nov. 2015.
[7] Y. Yu, G. Konstantinou, B. Hredzak and V. G. Agelidis, "Operation of Cascaded H-Bridge Multilevel Converters for Large-Scale Photovoltaic Power Plants Under Bridge Failures," **IEEE Trans. Ind. Electron.**, vol. 62, no. 11, pp. 7228–7236, Nov. 2015.
[8] G. Farivar, B. Hredzak and V. G. Agelidis, "Decoupled Control System for Cascaded H-Bridge Multilevel Converter Based STATCOM," **IEEE Trans. Ind. Electron.**, vol. 63, no. 1, pp. 322–331, Jan. 2016.
[9] X. Li, M. Su, Y. Sun, H. Dan and W. Xiong, "Modulation Strategy Based on Mathematical Construction for Matrix Converter Extending the Input Reactive Power Range," **IEEE Trans. Power Electron.**, vol. 29, no. 2, pp. 654–664, Feb. 2014.
[10] L. Sun, Z. Wu, F. Xiao, X. Cai and S. Wang, "Suppression of Real Power Back Flow of Nonregenerative Cascaded H-Bridge Inverters Operating Under Faulty Conditions," **IEEE Trans. Power Electron.**, vol. 31, no. 7, pp. 5161–5175, Jul. 2014.
[11] R. P. Aguilera, R. Baidya, P. Acuna, S. Vazquez, T. Mouton and V. G. Agelidis, "Model Predictive Control of Cascaded H-Bridge Inverters based on a Fast-Optimization Algorithm," in **Proc. IEEE IECON**, Yokohama, Japan, 2015, pp. 4003–4008.
[12] R. P. Aguilera, P. Lezana, G. Konstantinou, P. Acuna, B. Wu, S. Bernet and V. G. Agelidis, "Closed-Loop SHE-PWM Technique for Power Converters Through Model Predictive Control," in **Proc. IEEE IECON**, Yokohama, Japan, 2015, pp. 5261–5266.
[13] R. P. Aguilera, Y. Yu, P. Acuna, G. Konstantinou, C. D. Townsend, B. Wu and V. G. Agelidis, "Predictive Control Algorithm to Achieve Power Balance of Cascaded H-Bridge Converter," in **Proc. IEEE PRECEDE**, Valparaiso, Chile, 2015, pp. 49–54.